AMERICAN MUSEUM
Novitates

PUBLISHED BY THE AMERICAN MUSEUM OF NATURAL HISTORY
CENTRAL PARK WEST AT 79TH STREET, NEW YORK, N.Y. 10024
Number 2960, 16 pp., 14 figs. November 29, 1989

Description of the Embryonic Shell of *Nautilus belauensis* (Cephalopoda)

NEIL H. LANDMAN,[1] JOHN M. ARNOLD,[2]
AND HARRY MUTVEI[3]

ABSTRACT

This study describes several embryonic shells of *Nautilus belauensis* recovered from the Waikiki Aquarium during 1985–1986. They range in development from a prechambered caplike shell to a three-chambered shell. These shells confirm earlier studies that the cicatrix, the scarlike feature on the apex of the shell, is the site of initial shell formation. A multilayered calcareous deposit, known as the protoseptum, invests the interior of the shell apex. The microstructure of the first three septa and their mode of attachment to the outer shell wall are similar to that of septa in later stages of development. However, the proportions of the shell at these early embryonic stages are very different from those of postembryonic shells.

INTRODUCTION

Nautilus is the only living externally shelled cephalopod and, therefore, study of its embryology provides clues into that of extinct groups such as the ammonoids. However, the embryology of *Nautilus* was essentially unknown until the recovery of live embryos from the Waikiki Aquarium in 1985 (Arnold and Carlson, 1986; Arnold, 1987; Arnold et al., 1987). This paper summarizes observations on the development of the embryonic shell of *Nautilus belauensis* Saunders that were made subsequent to the publication of the

[1] Associate Curator, Department of Invertebrates, American Museum of Natural History.
[2] Research Associate, Department of Invertebrates, American Museum of Natural History; Professor, Pacific Biomedical Research Center, University of Hawaii, Honolulu, Hawaii 96822; Marine Biological Laboratory, Woods Hole, Mass. 02543.
[3] Curator, Swedish Museum of Natural History, 10405 Stockholm, Sweden.

 ISSN 0003-0082 / Price $2.35

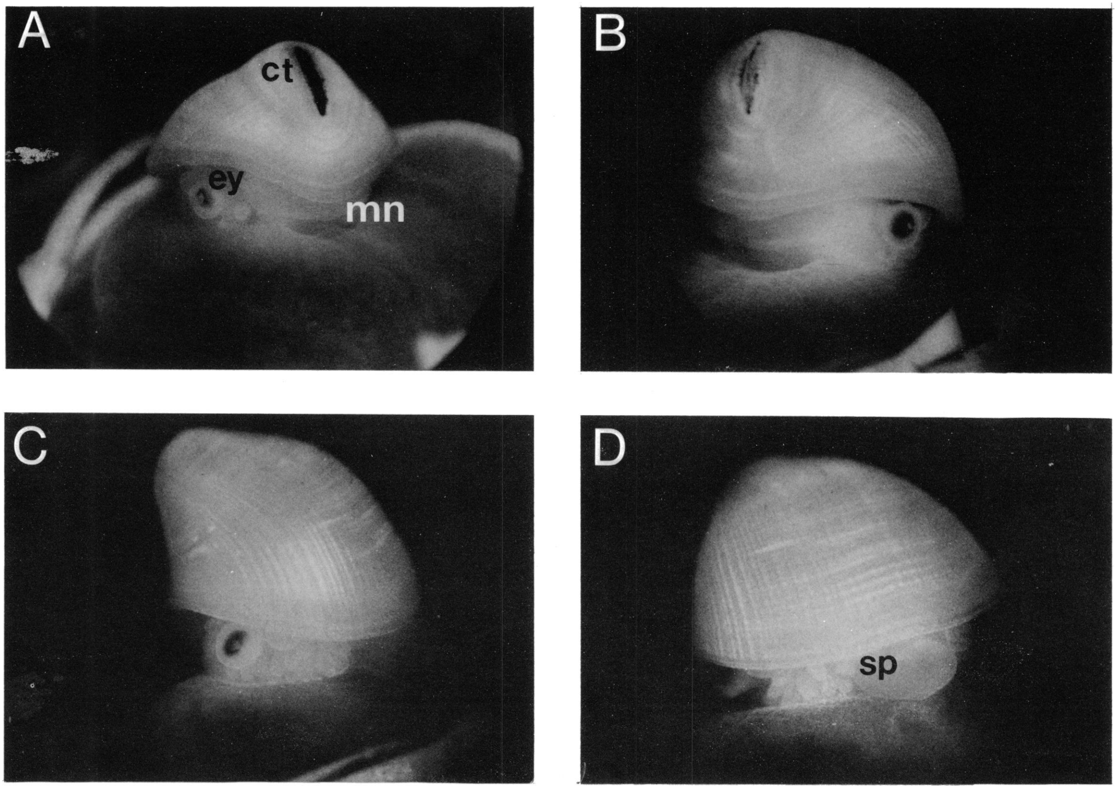

Fig. 1. Living embryo of *Nautilus belauensis* at the prechambered stage. The shell is approximately 3 mm maximum diameter. **A, B.** Three-quarter right and left views of cicatrix and dorsal region. **C.** Left view showing profile of shell. **D.** View of ventral region. ct, cicatrix; ey, eye; mn, mantle; sp, siphon.

initial description of the embryonic shell of this species in Arnold et al. (1987). We describe several embryos at different developmental stages ranging from the development of a prechambered caplike shell to the development of a three-chambered shell. Although the number of specimens is small, they are unique and, therefore, merit serious study. They were recovered from eggs in the Waikiki Aquarium during 1985–1986 and are presently stored in Arnold's laboratory at the University of Hawaii. We will treat the gross morphology of the embryonic shell in this paper and reserve description of the soft tissues for another paper.

Acknowledgments

John Arnold gratefully acknowledges the support of the Grass Foundation, the *Nautilus* Research Corporation, the Hawaiian Malacological Society, the Friends of the Waikiki Aquarium, and the *Teuthis obscura* Fund. We thank John A. Chamberlain, Jr. (Brooklyn College) and W. Bruce Saunders (Bryn Mawr College) for their helpful reviews of the manuscript. Andrew S. Modell and Peling Fong (AMNH) helped prepare figures 8–10, 12, and 13. Lennart Alex Anderson (Swedish Museum of Natural History) prepared figure 11. Stephanie Crooms (AMNH) word-processed the manuscript.

Material

The shells described are from live embryos or from animals that were already dead when the egg cases were opened. The embryos were fixed in 2.6 percent gluteraldehyde-seawater buffered to pH 7.4, rinsed in seawater, and postfixed in 1 percent osmium tetroxide. Altogether, we examined four shells: two pre-

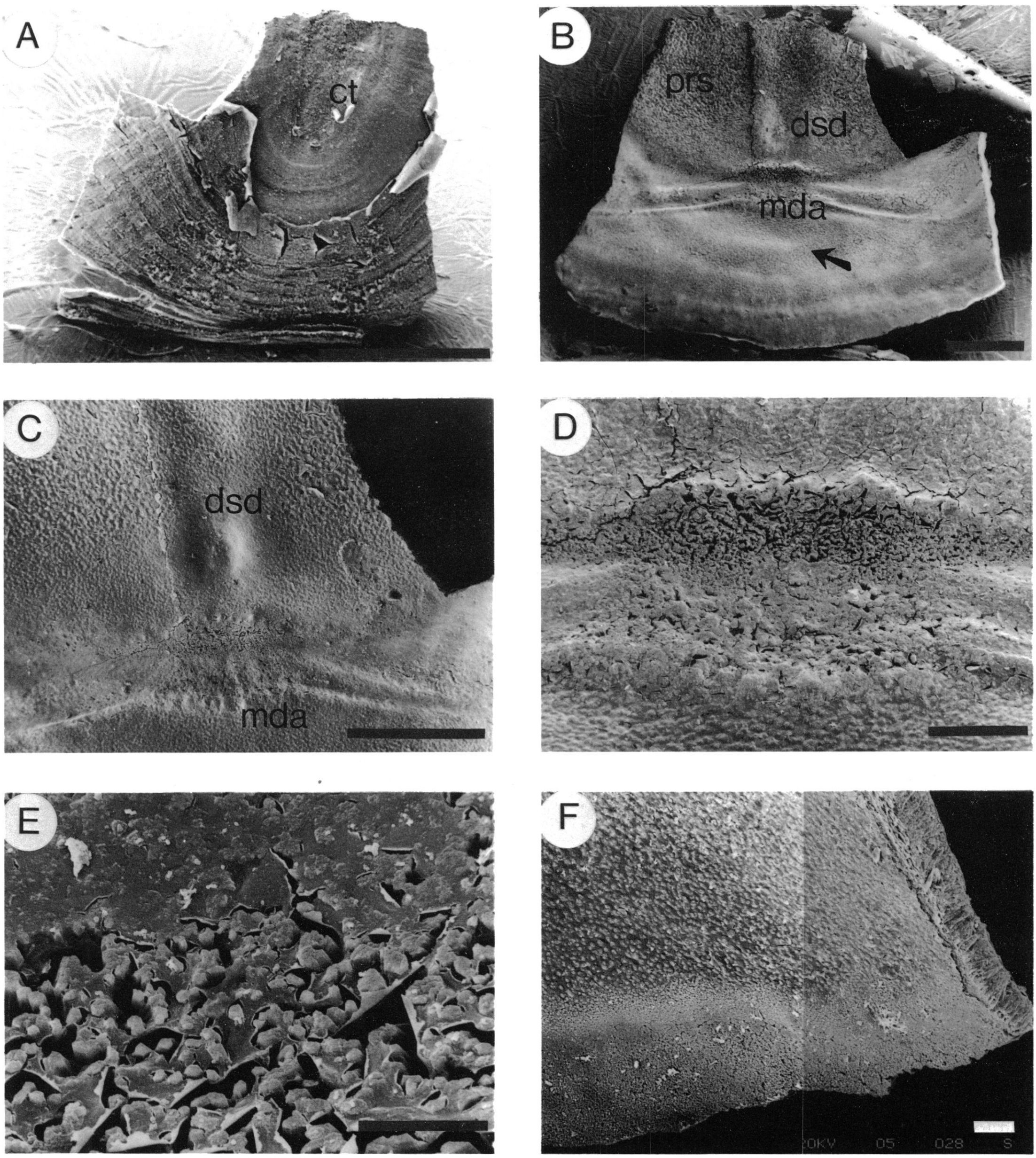

Fig. 2. Cicatrix region and interior of shell apex of embryo illustrated in figure 1. Dorsal direction is toward bottom. **A.** Cicatrix (ct) and dorsal region. Scale bar = 1 mm. **B.** Interior view of A showing protoseptum (prs), dorsal septal depression (dsd), middorsal area (mda), and dorsal edge. The curved elevation (arrow) corresponds to a deep concentric depression on the outside of shell. A linear crack has developed parallel to the cicatrix. Scale bar = 400 μm. **C.** Close-up of dorsal septal depression and middorsal area. Scale bar = 400 μm. **D.** Close-up of middorsal area located between nacreous protoseptum and zone of nacreous secretion. Scale bar = 100 μm. **E.** Close-up of prismatic structure of middorsal area. Scale bar = 20 μm. **F.** View of dorsal margin showing transition from nacreous to prismatic secretion. Scale bar = 40 μm.

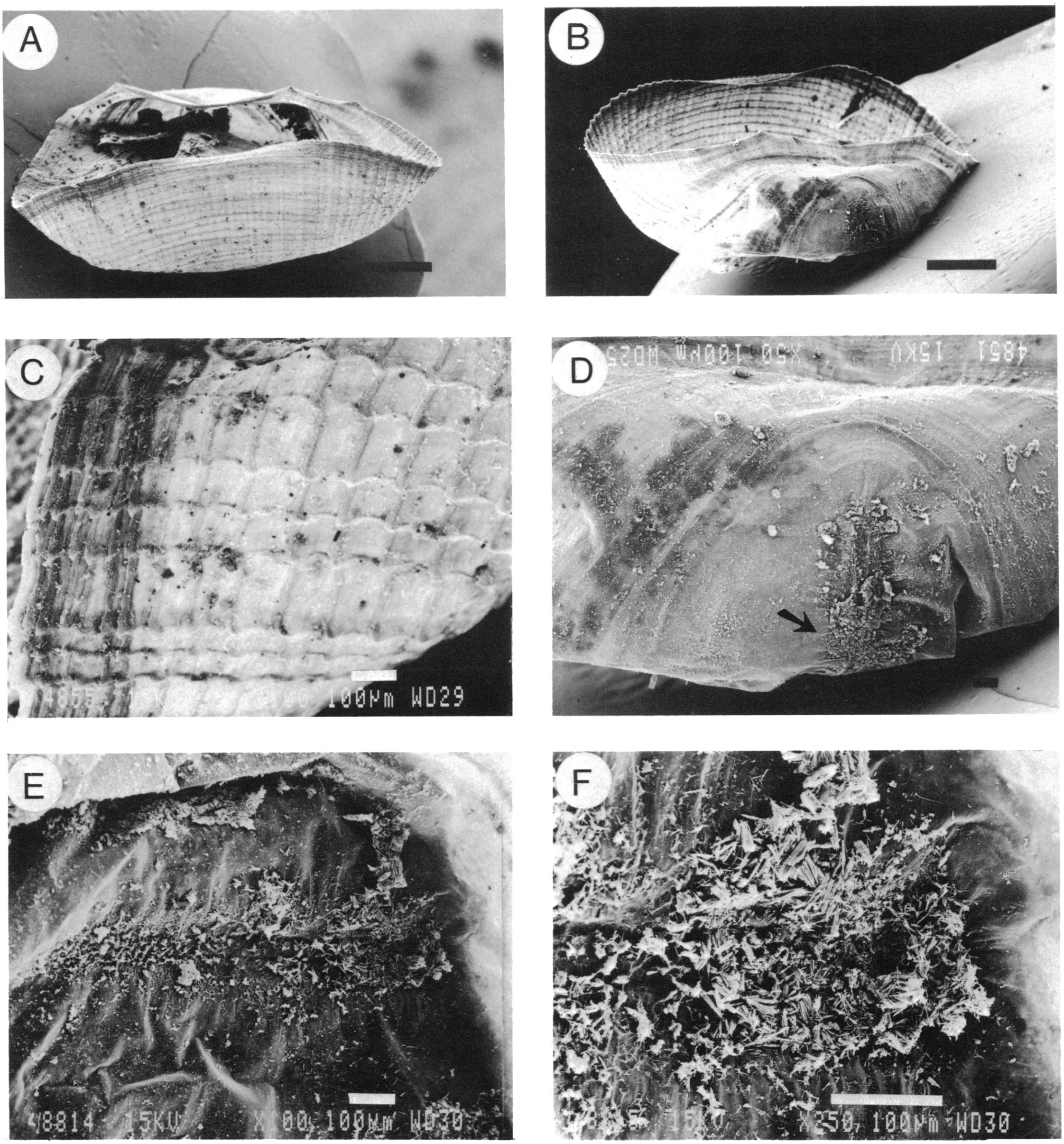

Fig. 3. Partially decalcified shell at the prechambered stage. This specimen is nearly transparent and has lost its original shape. It was only lightly coated to obtain micrographs A–D. **A.** View looking over ventral edge into interior of shell. Scale bar = 1 mm. **B.** Cicatrix region and interior of shell. Scale bar = 1 mm. **C.** Reticulate ornamentation. The "growth lines" become approximated as they approach the aperture (toward the left), possibly reflecting stress just prior to death. Scale bar = 100 μm. **D.** Cicatrix region showing central bar and undulations of periostracum (arrow). The dorsal part of the cicatrix is toward the top. Scale bar = 100 μm. **E.** Interior view of cicatrix. The dorsal direction is to the right. Scale bar = 100 μm. **F.** Close-up of dorsal septal depression. Scale bar = 100 μm.

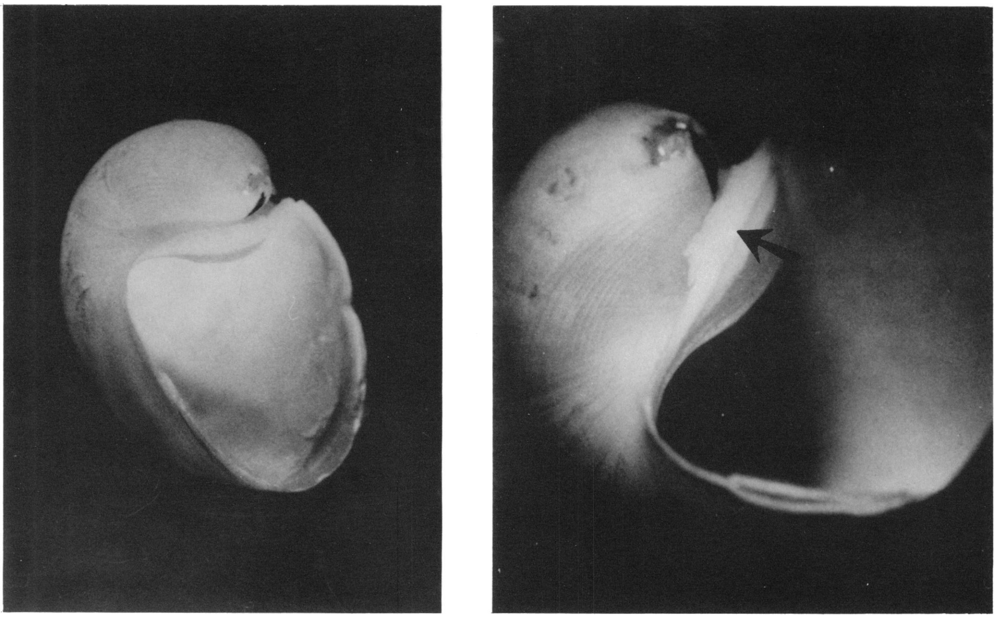

Fig. 4. Two views of the two-chambered shell showing reflected dorsal lip (arrow). The shell is approximately 10.3 mm maximum diameter. There is a small nick in the shell near the cicatrix due to handling.

chambered [one partially decalcified and the other originally described in Arnold et al. (1987)], one two-chambered, and one three-chambered. Shells were preserved in 95 percent ethyl alcohol. They were critically point dried and coated with gold or gold palladium for scanning electron microscopy.

RESULTS

Prechambered Shell

The prechambered shell illustrated in figure 1 is approximately 3 mm maximum diameter and 0.17 whorl angular length (60°). It was previously described as an embryo at the one-chambered stage of development (Arnold, 1987: figs. 4, 5; Arnold et al., 1987: figs. 1B, 2–7, 9, 10; Saunders and Landman, 1987: pl. IV; Arnold, 1988: figs. 6–11). Because this specimen has not yet formed its first septum, we will refer to it henceforth as prechambered. The apex is cap-shaped. The ventral part of the shell is curved but the dorsal part flat. The shell margin is fairly straight near the siphon but slightly incurved near the eye. The dorsal edge is only slightly reflected backward.

The interior of the apex is covered with the protoseptum, composed mostly of nacre (fig. 2B). The morphology of the shell interior partly reflects that of the exterior. For example, a circular depression called the dorsal septal depression occurs in the protoseptum and corresponds to the dorsal circular terminus of the cicatrix (fig. 2B, C; see also Arnold et al., 1987). A curved elevation is also visible on the shell interior near the aperture, which corresponds to a deep concentric depression on the outside (fig. 2B). In addition to these features, a broad porous region called the middorsal area occurs at the dorsal margin of the protoseptum (fig. 2B, C, D, E). Two lateral ridges extend outward from each side of this area, which is covered with prismatic crystals and is quite distinct from the nacreous surface of the protoseptum. A zone of nacreous secretion occurs adoral of the middorsal area followed by a zone of prismatic secretion (fig. 2F).

A partially decalcified specimen at this same stage of development permits additional observations of the cicatrix region and formation of the ornamentation (fig. 3). This specimen is mostly composed of periostracum

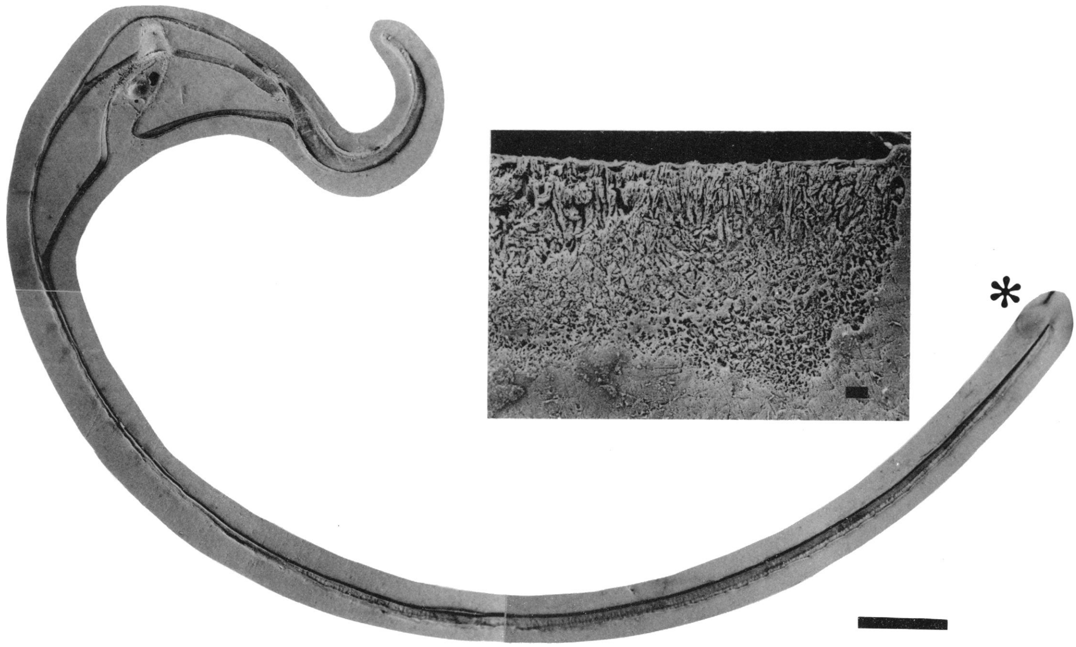

Fig. 5. Parasagittal cross section through the two-chambered shell illustrated in figure 4. The angular length of its body chamber equals approximately 180°. Scale bar = 1 mm. Inset: Close-up of ventral edge, which is composed almost entirely of the outer prismatic layer (asterisk). Scale bar = 10 μm.

with a few pieces of shell still attached. It is nearly transparent and has lost its original shape. The cicatrix is surrounded by a shallow lenticular depression enclosed in an outer ridge (fig. 3B, D). The cicatrix consists of a central bar with circular termini at each end as previously described (Arnold et al., 1987; Arnold, 1988). The periostracum exhibits a series of low undulations that radiate outward from the central bar. In the shell interior, the cicatrix appears as an elongate depression with ovoid expansions at each end (fig. 3E, F). The ornamentation of the shell consists of prominent lines that diverge from the apex and others that parallel the aperture (fig. 3A, B, C). These latter lines ("growth lines") become approximated and darker as they approach the aperture possibly indicating stressful conditions and a consequential deceleration in the rate of growth prior to death (fig. 3C).

Two-Chambered Shell

This stage of development is represented by one specimen (figs. 4–9). It is 10.3 mm maximum diameter and consists of 0.63 whorl (227°). The angular length of its body chamber equals approximately 180°. All of these measurements are approximate because they were taken from a parasagittal cross section. The dorsum is much more recurved than it is at the prechambered stage of development (figs. 4–6, 8). Due to handling, there is a small nick in the shell near the cicatrix and the ventral edge is slightly broken.

Cross sections reveal the microstructure of the shell wall, siphuncle, and septa. Near the distal end of the siphuncle (caecum), the shell wall consists of the outer prismatic layer of the shell wall proper and the outer prismatic, nacreous, and inner prismatic layers of the

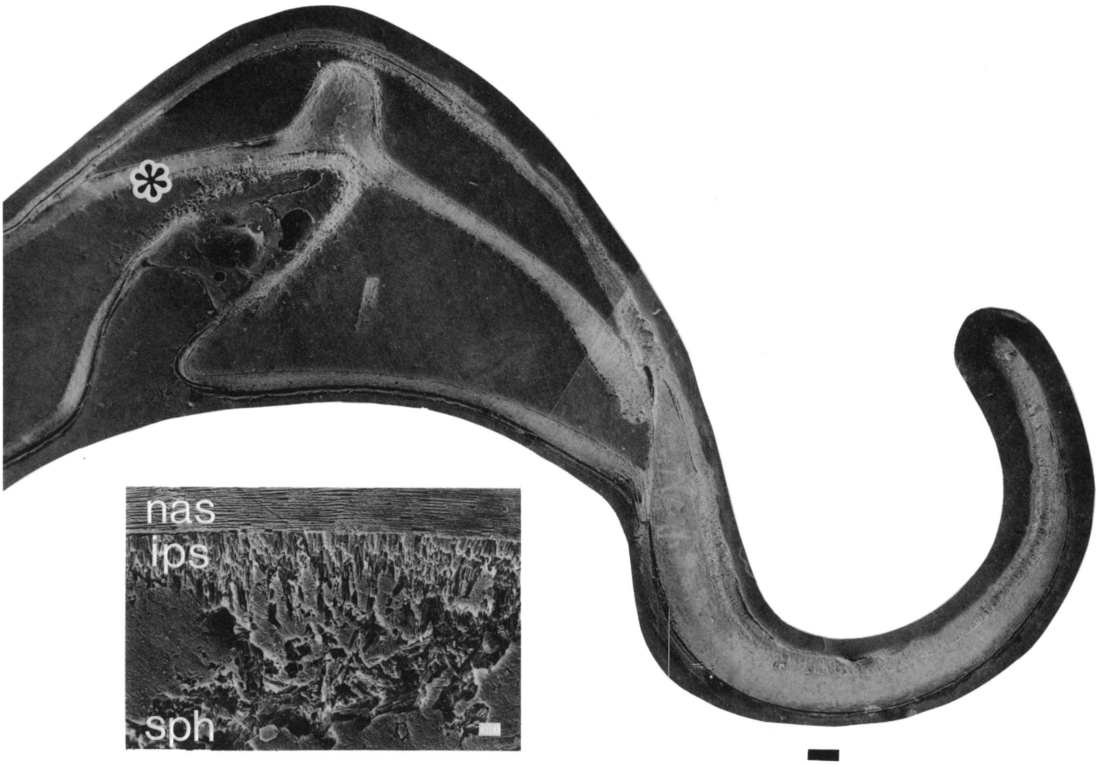

Fig. 6. Parasagittal cross section through the phragmocone of the two-chambered shell illustrated in figures 4 and 5 showing siphuncle and first two septa. Scale bar = 100 μm. Inset: Close-up of attachment of first septum to siphuncle (asterisk). nas, nacreous layer of first septum; ips, prismatic layer of first septum on its adoral side; sph, spherulitic prismatic layer of siphuncle. Scale bar = 10 μm.

protoseptum (figs. 6, 7A). The dorsal end of the protoseptum is visible adapical of the junction of the first septum and shell wall on the dorsal side (figs. 8A, 9). The thick nacreous layer of the protoseptum terminates in an area of coarse spicular crystals. The dorsum is three-layered and consists of the outer prismatic, nacreous, and inner prismatic layers of the shell wall proper (figs. 6, 8A). The nacreous layer attains it maximum thickness, approximately 275 μm, just adoral of the attachment of the second septum to the shell wall. The nacreous layer thins adapturally so that the dorsal tip of the shell consists only of the outer prismatic layer (fig. 8B, C).

On the ventral side, the protoseptum tapers out adapical of the attachment of the first septum to the shell wall (fig. 6). The venter, like the dorsum, is three layered. First the inner prismatic, then the nacreous layer disappears toward the aperture. The ventral edge is composed almost entirely of the outer prismatic layer. However, because the edge is slightly broken back a thin layer of nacre is also present (fig. 5). The structure of the outer prismatic layer of the ventral edge is more spherulitic-dendritic than that of the dorsal edge because the ventral edge is growing faster.

The structure of the distal end of the siphuncle and its attachment to the first septum is illustrated in a parasagittal section (figs. 6, 7A, B). The siphuncle consists of an outer spherulitic prismatic layer that extends to the inner layer of the protoseptum and an inner conchiolin layer. The siphuncle is attached to the septal neck of the first septum, which

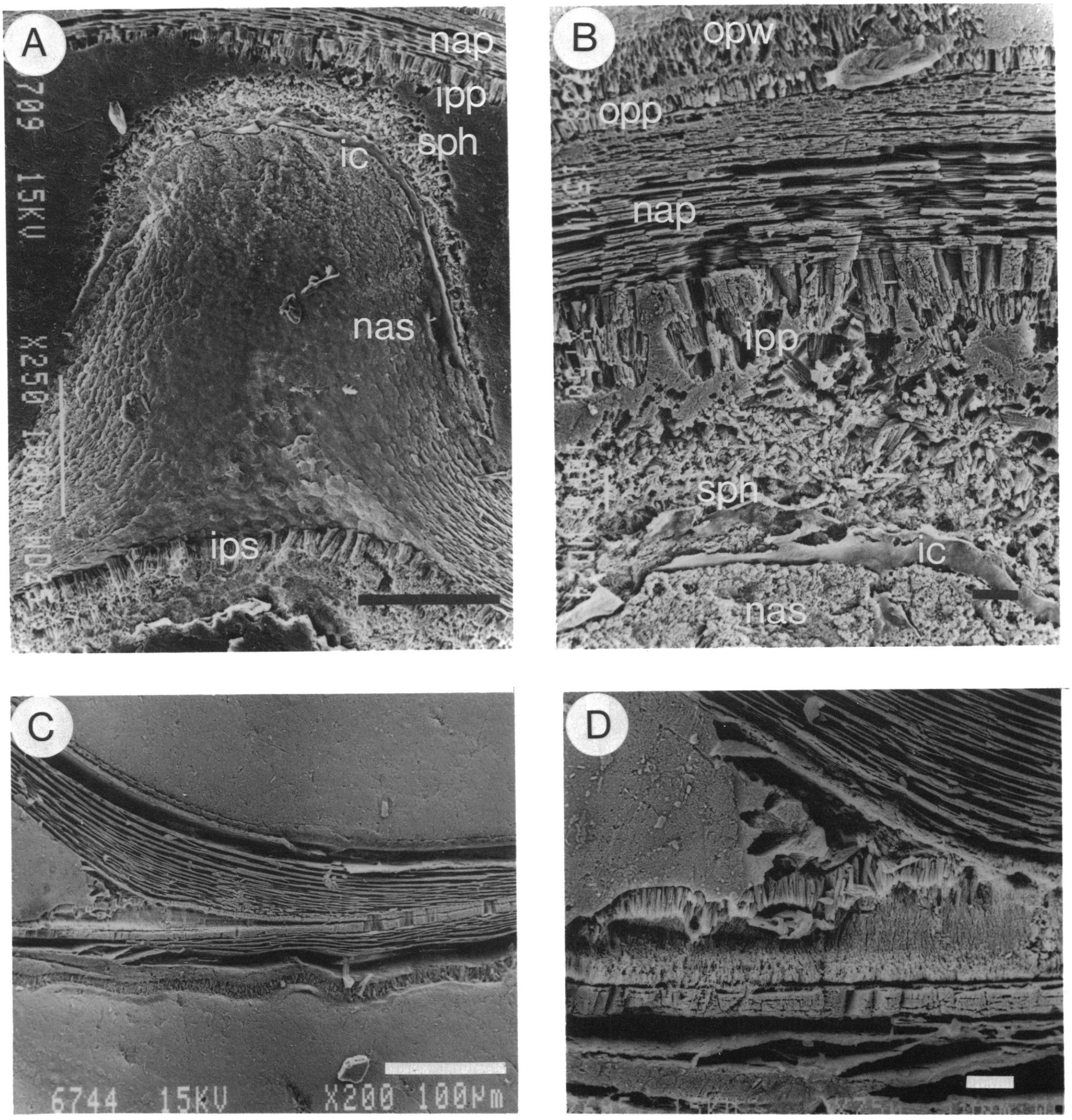

Fig. 7. Parasagittal cross section through phragmocone of the two-chambered shell illustrated in figures 4–6 showing enlargements of distal end of siphuncle and junction of second septum and ventral shell wall. **A.** Distal end of siphuncle. Because this is a parasagittal section, the nacreous and inner prismatic layers of the septal neck are broadly exposed. nap, nacreous layer of protoseptum; ipp, inner prismatic layer of protoseptum; sph, spherulitic-prismatic layer of siphuncle; ic, inner conchiolin layer of siphuncle; nas, nacreous layer of septal neck of first septum; ips, inner prismatic layer of septal neck of first septum. Scale bar = 100 μm. **B.** Close-up of the structure of apical part of shell wall and distal end of siphuncle. opw, opp, outer prismatic layers of wall proper and protoseptum, respectively; nap, nacreous layer of protoseptum; ipp, inner prismatic layer of protoseptum; sph, spherulitic prismatic layer of siphuncle; ic, inner conchiolin layer of siphuncle; nas, nacreous layer of septal neck of first septum. Scale bar = 10 μm. **C.** Junction of second septum and ventral shell wall. Cements composed of prismatic crystals appear on the adapical side of the septum. The prismatic layer from the adapical side of the septum continues adorally along the inside of shell wall. Scale bar = 100 μm. **D.** Close-up of cements on adapical side of second septum. Scale bar = 10 μm.

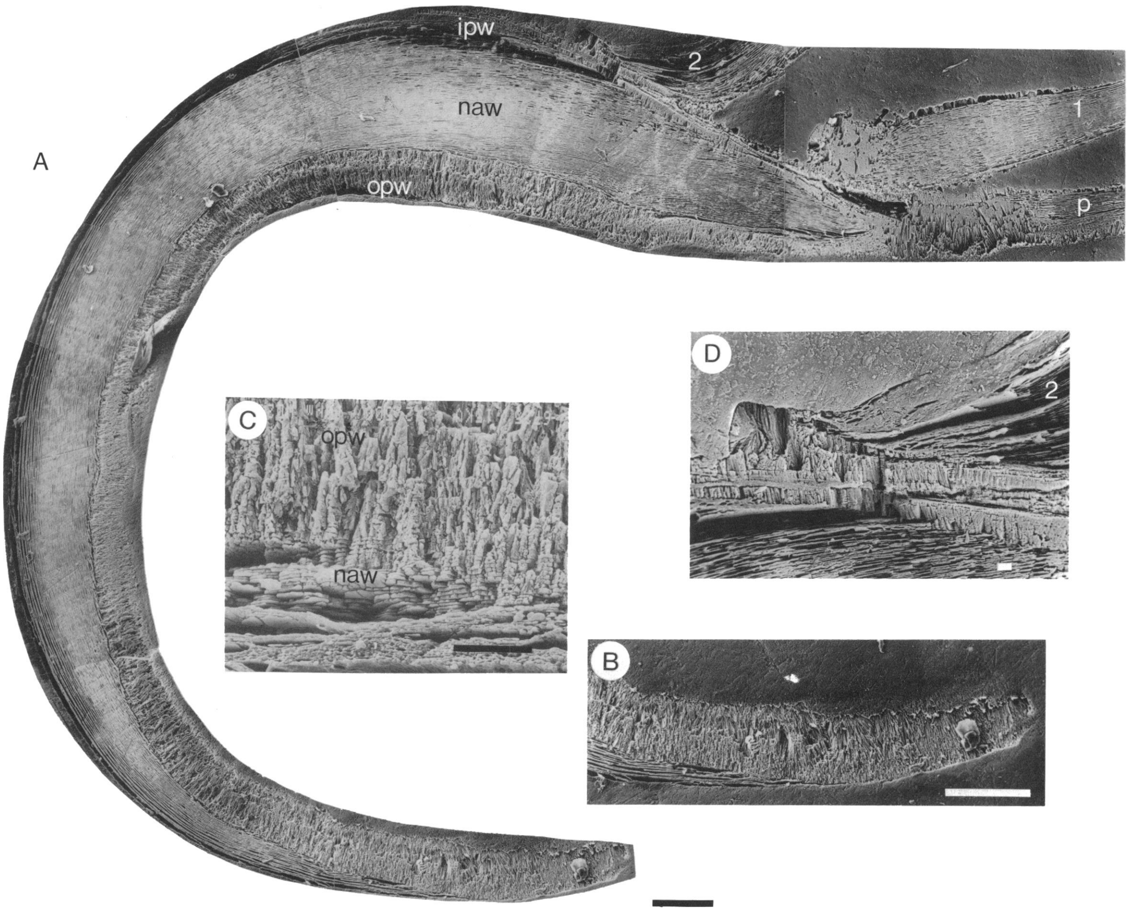

Fig. 8. Parasagittal cross section through dorsal region of the two-chambered shell illustrated in figures 4–7 showing part of the protoseptum (p) and the first two septa (1, 2). **A.** Dorsum of shell consists of outer prismatic (opw), nacreous (naw), and inner prismatic (ipw) layers of shell wall proper. Scale bar = 100 μm. **B.** Close-up of dorsal edge, which only consists of outer prismatic layer. Scale bar = 10 μm. **C.** Structure of shell wall a small distance from the dorsal edge. Scale bar = 10 μm. **D.** Close-up of the junction of the second septum and dorsal shell wall. Prismatic crystals occur on both the adapical and adoral sides of the septum and may represent septal cements. Scale bar = 10 μm.

consists, in turn, of an outer spherulitic prismatic layer (on its adapical side), a thick nacreous layer that is structurally modified distally, and an inner prismatic layer (on its adoral side). Because this is a parasagittal section, the nacreous and inner prismatic layers of the septal neck are broadly exposed. Nevertheless, the structure of the distal end of the siphuncle and its attachment to the first septum are similar to that illustrated in Arnold et al. (1987; fig. 20F) based on a cross section through the early whorls of an adult specimen of *Nautilus pompilius* (see also Mutvei, 1972: fig. 2).

The attachment of the septa to the shell wall is visible in figures 7C, D, 8A, D, and 9. At the junction of the first septum and dorsal shell wall, a layer of prismatic crystals occurs adapical of the septum (figs. 8A, 9). This may represent a thicker part of the inner prismatic layer of the protoseptum or a cement associated with the septum, which commonly occurs on the septa of older specimens (Grégoire, 1987). The first septum terminates

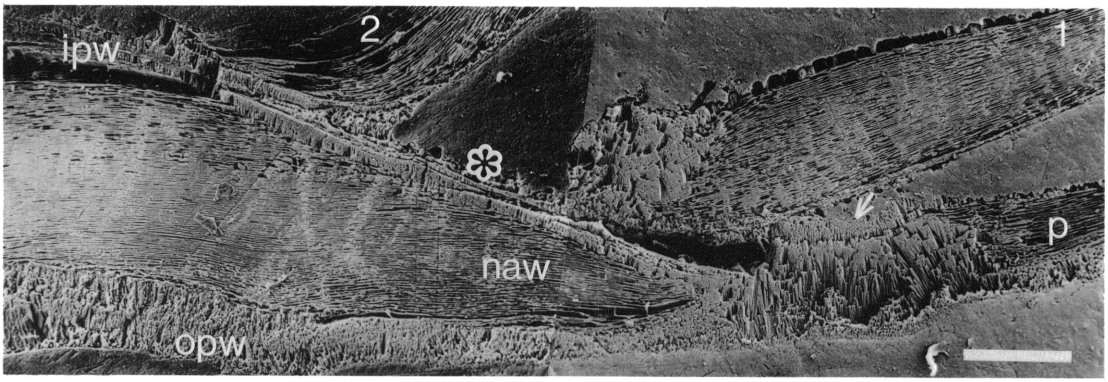

Fig. 9. Enlargement of the junction of first two septa (1, 2) and dorsal wall of the two-chambered shell illustrated in figures 4–8. The adoral direction is toward the left. At the junction of the first septum and dorsal wall, a layer of prismatic crystals (arrow) occurs adapical of the septum. The septum terminates in an area of coarse spicular crystals. Adoral of this septum, a thin prismatic layer (asterisk) appears inside the inner prismatic layer of the shell wall proper. At the junction of the second septum and the dorsal wall, prismatic crystals occur on both the adapical and adoral sides of the septum. p, protoseptum; opw, outer prismatic layer of shell wall proper; naw, nacreous layer of shell wall proper; ipw, inner prismatic layer of shell wall proper. Scale bar = 100 μm.

in an area of coarse spicular crystals. Adoral of the first septum, a thin prismatic layer appears inside the inner prismatic layer of the shell wall proper. Based on the structure of septa in older specimens, this layer may represent either a continuation of the prismatic layer of the first septum from its adapical side (Blind, 1976) or a continuation of the cement from its adapical side (Grégoire, 1987). At the junction of the second septum and the dorsal wall, prismatic crystals occur on both the adapical and adoral sides of the septum and may represent septal cements (figs. 8A, D, 9; Grégoire, 1987). Adoral of this septum, a prismatic layer appears inside the inner prismatic layer of the shell wall and, as in the first septum, may represent a continuation of the prismatic layer of the second septum from the adapical side or a continuation of the cement from its adapical side. At the junction of the septa and ventral shell wall, similar septal cements composed of prismatic crystals occur on the adapical side of the septa (fig. 7C, D). The prismatic layers from the adapical side of the septa also continue adorally along the inside of the shell wall.

Three-Chambered Shell

This stage of development is represented by one specimen (figs. 10–13, 14C). It is 13.0 mm maximum diameter and consists of 0.65 whorl (234°). The angular length of its body chamber equals approximately 155°. All of these measurements are approximate because they were taken from an X-ray. When this specimen was opened after removal from the egg capsule, liquid was present in its chambers. It also had a jaw and radula. This specimen permits several observations of the dorsal region, the attachment of the septa to the shell wall and siphuncle, and the interior of the body chamber.

The dorsal region is well developed and in cross section reveals a thick nacreous layer in addition to the inner and outer prismatic layers (fig. 10B, C). The nacreous layer is approximately 230 μm thick just adoral of the

→

Fig. 10. Three views of the three-chambered shell. **A.** Parasagittal cross section of part of phragmocone showing recurved dorsal region, siphuncle, and first three septa (1, 2, 3). This specimen was broken to

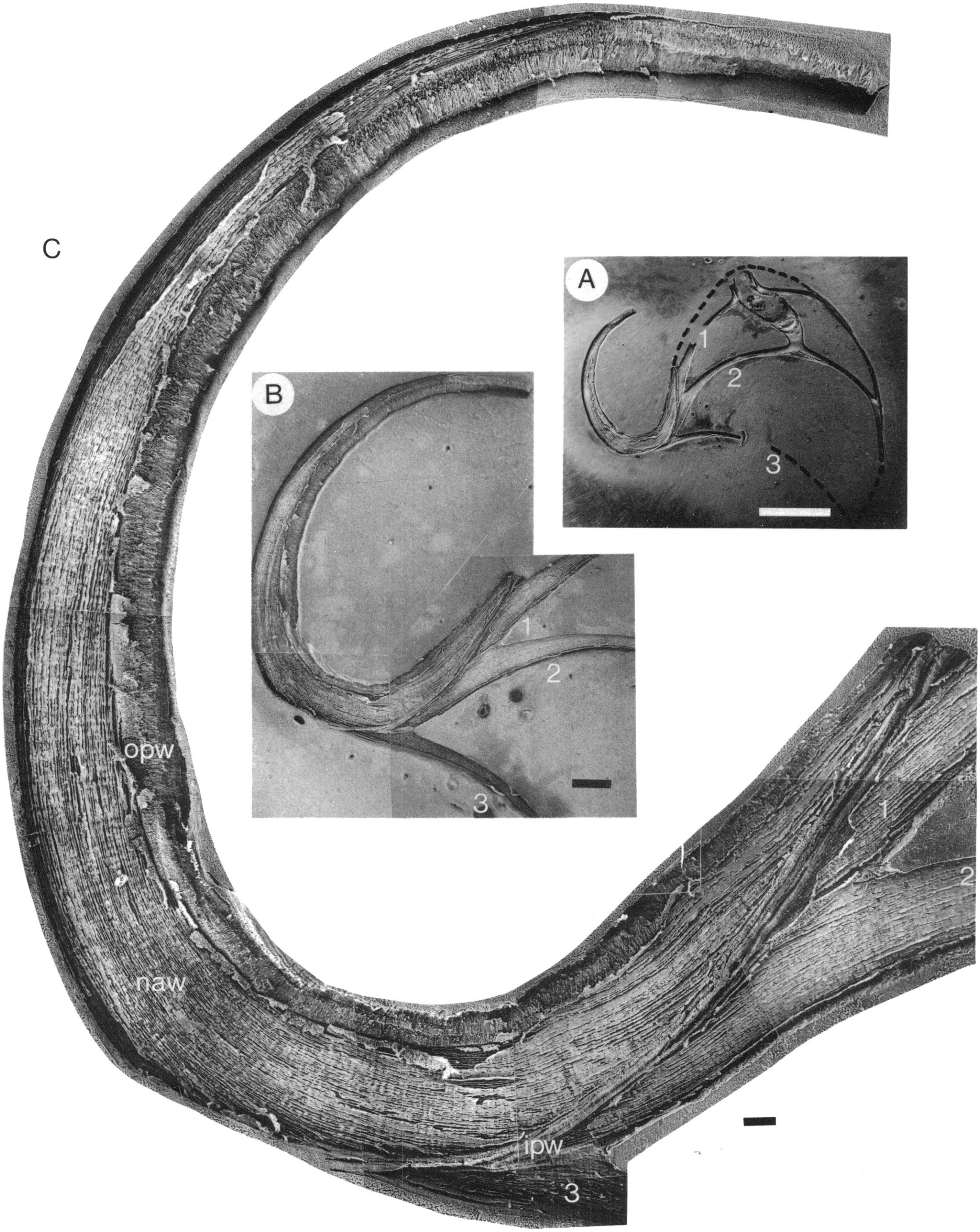

permit examination of the body chamber interior, and the outlines of the missing portions of the shell are indicated by dashes. Scale bar = 500 μm. **B.** Close-up of dorsal region and first three septa in A. The cross section is parasagittal and, as a result, the third septum rests partly on the second septum, and the second septum, in turn, rests partly on the first. Scale bar = 200 μm. **C.** Enlargement of dorsal region showing outer prismatic (opw), nacreous (naw), and inner prismatic (ipw) layers of the shell wall. Scale bar = 50 μm.

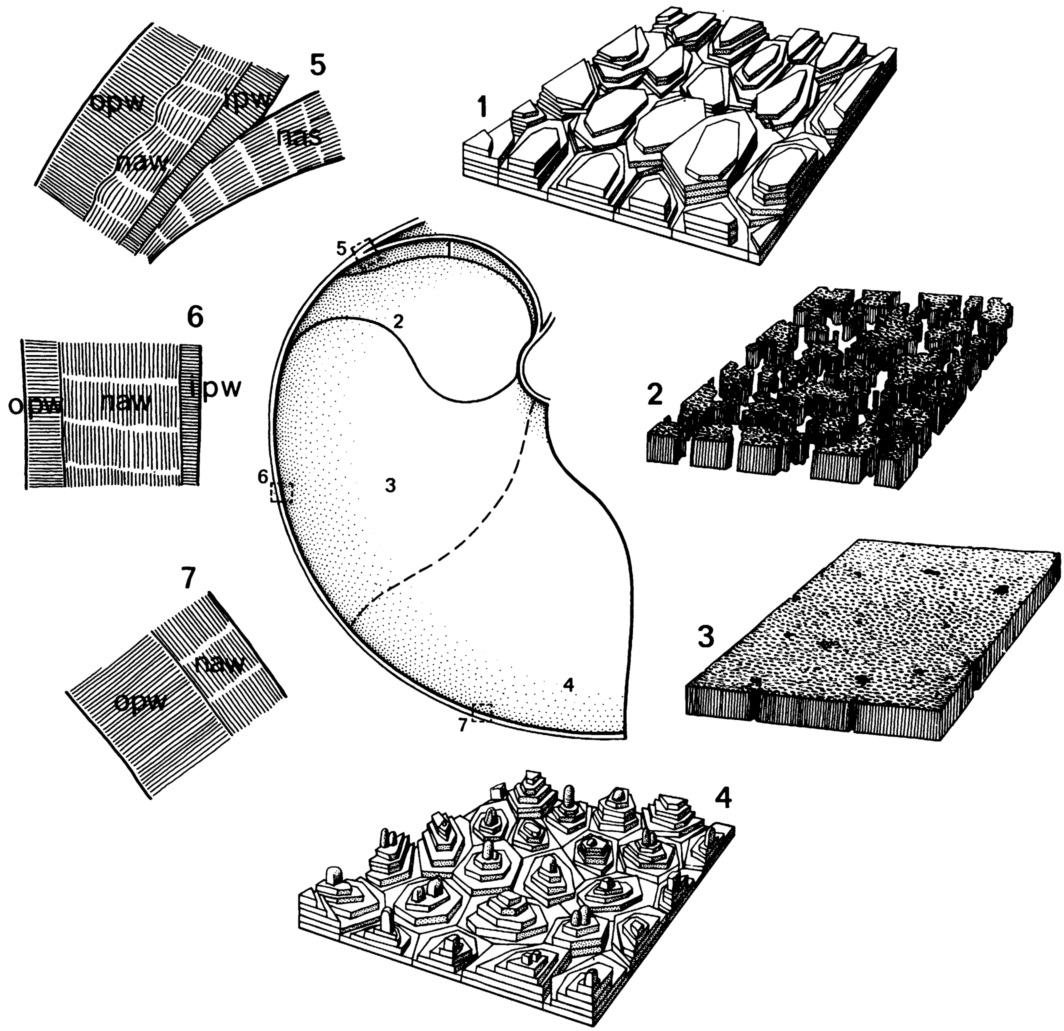

Fig. 11. Cutaway of the three-chambered shell minus its phragmocone showing the interior of the left-hand portion of the body chamber from the third septum (near 1) to the broken edge of the apertural margin (near 4). The scar of the retractor muscle (near 2) is also visible. The dashed line marks the transition from the zone of prismatic to that of nacreous secretion. The dorsal direction is toward the right. The different regions of shell secretion are represented by close-ups as follows: (1) nacreous crystals of the third septum, (2) inner prismatic layer, (3) inner prismatic layer several mm farther forward, and (4) nacreous crystals of nacreous layer of shell wall. These close-ups appear as micrographs in figure 12A–D. The structure of the outer wall is also illustrated in diagrammatic cross sections along the shell edge as follows: (5) junction of third septum and shell wall showing nacreous layer of septum (nas) and inner prismatic (ipw), nacreous (naw), and outer prismatic (opw) layers of shell wall, (6) three-layered shell wall, and (7) nacreous and outer prismatic layers of shell wall near apertural edge. These diagrams appear as micrographs in figure 13A–D.

attachment of the third septum. The dorsum is reflected further backward toward the apex than it is at the two-chambered stage of development. The dorsal edge consists entirely of the outer prismatic layer.

The attachment of the septa to the dorsal shell wall is visible in cross section (fig. 10A, B, C). This cross section is parasagittal and, as a result, the third septum rests partly on the second septum, and the second septum,

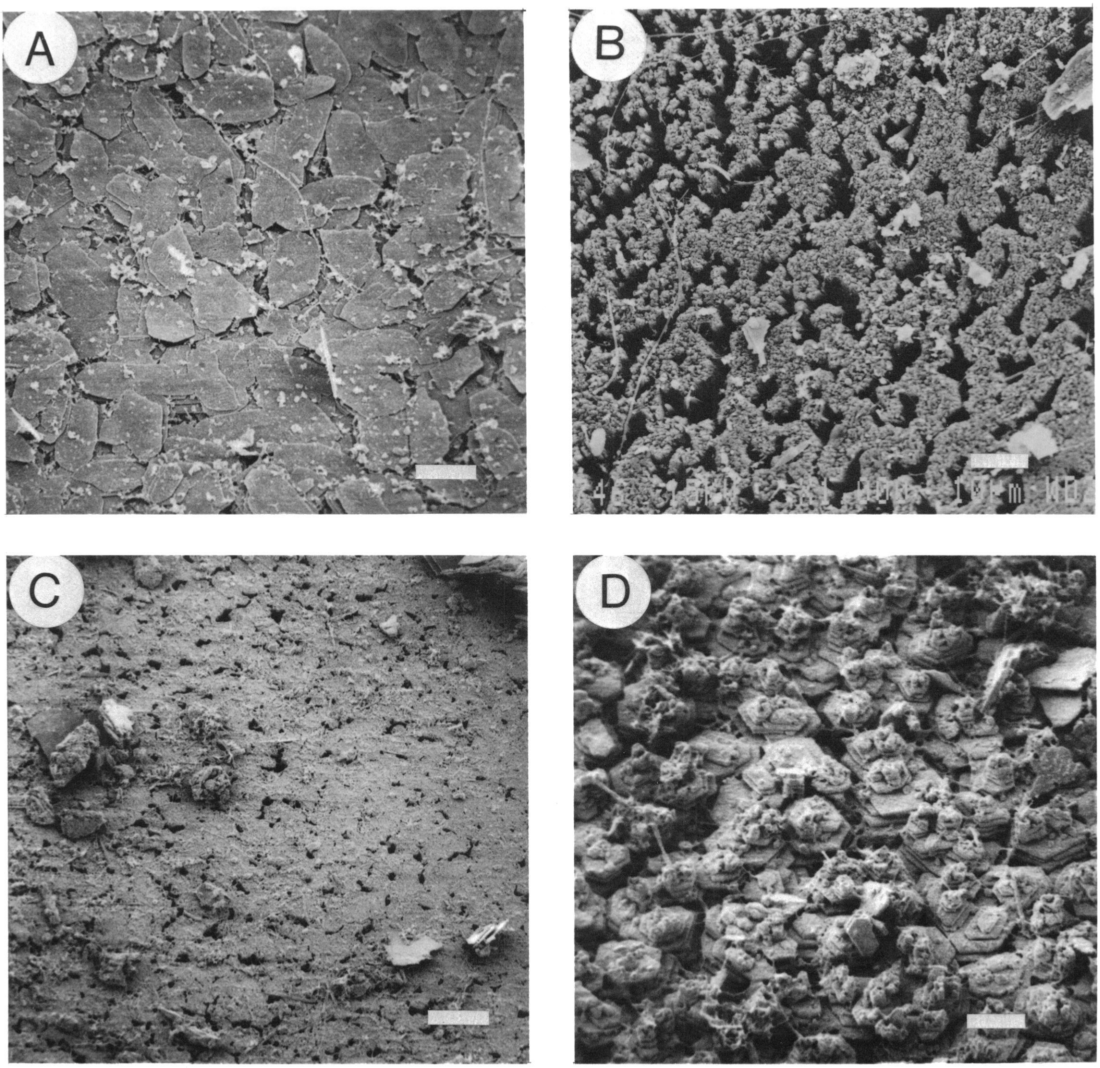

Fig. 12. Close-ups of interior surface of body chamber of the three-chambered shell as illustrated in figure 11. **A.** Nacreous crystals of third septum (represented in fig. 11.1). Scale bar = 10 μm. **B.** Inner prismatic layer just adoral of third septum (represented in fig. 11.2). Scale bar = 10 μm. **C.** Inner prismatic layer several mm adoral of B (represented in fig. 11.3). Scale bar = 10 μm. **D.** Nacreous crystals near broken edge of apertural margin (represented in fig. 11.4). Scale bar = 5 μm.

in turn, rests partly on the first. Cements composed of prismatic crystals occur on the adapical side of the junction of the septa and shell wall. In addition, the prismatic layers from the adapical sides of the septa may continue adorally along the inside shell wall. The wedge of prismatic crystals just adapical of the third septum is also visible in three-dimensional view in figure 13A.

We examined the interior surface and structure of the body chamber wall from the third septum to just short of the aperture (figs. 11–13). The structure of the wall is visible along a broken edge. The wall near the site of attachment of the third septum consists of three layers, excluding the periostracum (figs. 11.5, 13A). The surface of the third septum is covered with nacreous tablets (figs. 11.1,

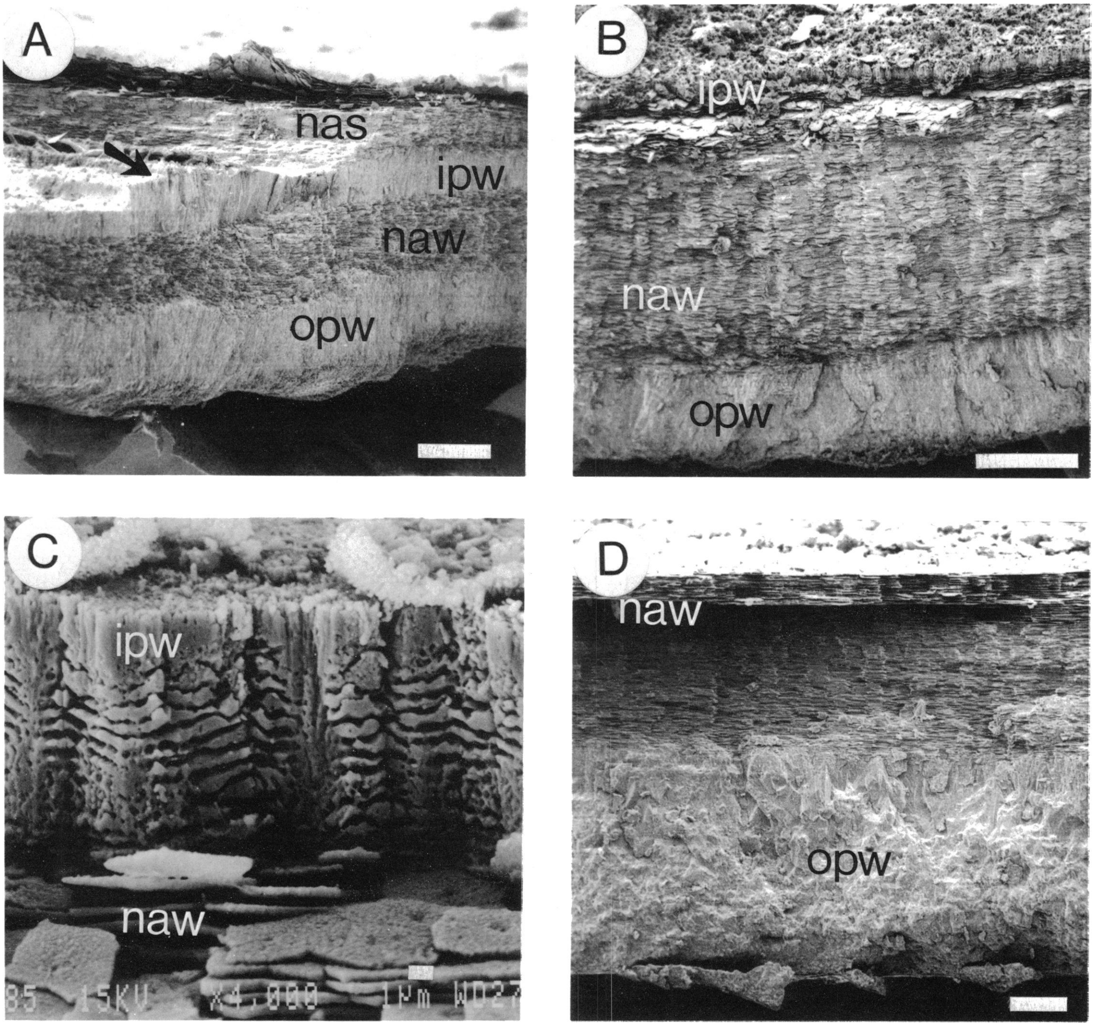

Fig. 13. Microstructure of outer wall of body chamber of the three-chambered shell as illustrated in figure 11. **A.** Junction of the third septum and ventral shell wall showing the nacreous layer of the septum (nas), the wedge of prismatic crystals (arrow) just adapical of the septum, and the inner prismatic (ipw), nacreous (naw), and outer prismatic (opw) layers of the outer wall (represented in fig. 11.5). Scale bar = 50 μm. **B.** Three-layered shell wall excluding periostracum (represented in fig. 11.6). Scale bar = 50 μm. **C.** Close-up of inner prismatic layer and transition to nacreous layer below. Scale bar = 1 μm. **D.** Shell wall near apertural edge only consists of nacreous and outer prismatic layers (represented in fig. 11.7). Scale bar = 20 μm.

12A). An area of prismatic crystals extends approximately 7.5 mm in front of this septum (figs. 11-2, 11-3, 12B, C). The scars of the retractor muscle and subepithelial musculature are also visible. The surface of the inner prismatic layer is marked by numerous pores, some of which occur in bands. These pores may have housed epithelial extensions of the mantle and muscle, thereby strengthening the attachment to the shell wall. The crystals of the inner prismatic layer show a transition to the tablets of the nacreous layer below (fig. 13C). The area of nacreous secretion extends approximately 6 mm to the broken edge of

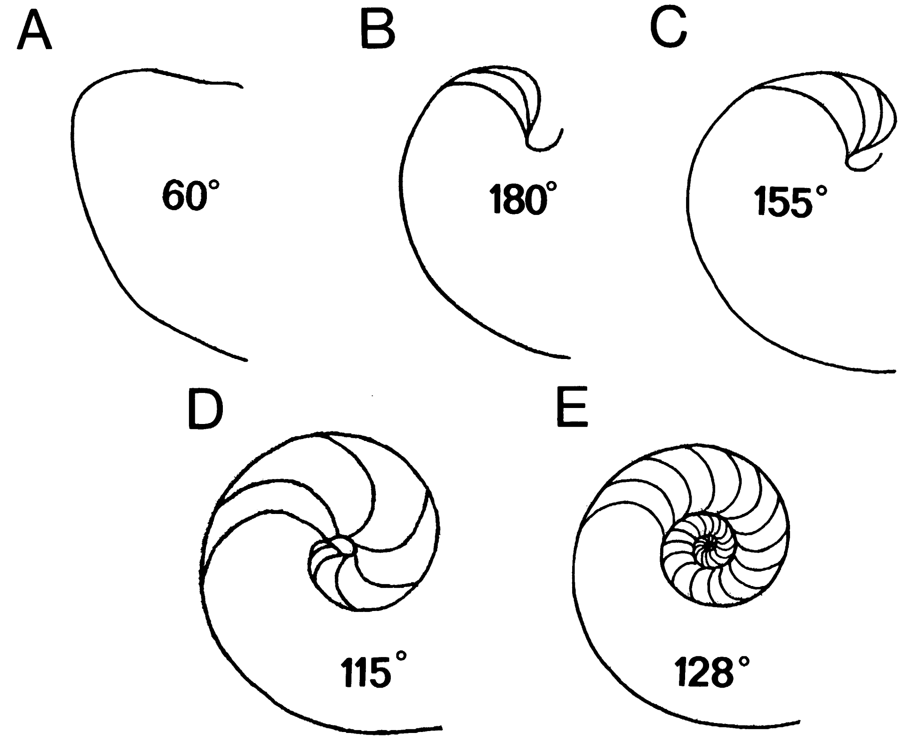

Fig. 14. Median cross sections of five specimens of *Nautilus belauensis* and *N. pompilius* at different ontogenetic stages portrayed at the same size showing the differences in the angular length of the body chamber. The siphuncle is omitted for simplification. **A.** Prechambered shell of *N. belauensis,* 3 mm diameter. **B.** Two-chambered shell of *N. belauensis,* 10.3 mm diameter. **C.** Three-chambered shell of *N. belauensis,* 13 mm diameter. **D.** Eight-chambered shell of *N. pompilius,* 25 mm diameter. **E.** Adult shell of *N. belauensis* with 35 septa, 220 mm diameter.

the apertural margin (figs. 11.4, 12D). Prismatic crystals are beginning to form on the surface of the nacreous crystals of this layer.

DISCUSSION

The shape of the shell of *Nautilus belauensis* changes markedly during embryogenesis (fig. 14). The shapes at the two- and three-chambered stages of development are very different from that of the postembryonic shell. For example, the body chamber at the two-chambered stage is much longer than it is in juveniles. In addition, the ratio of phragmocone to body-chamber volume is very low, implying that the animal could not have been neutrally buoyant at this stage. Clearly, the proportions of these embryonic animals are very different from those of later ontogenetic stages. However, the shape of the shell approaches that of juveniles in late embryogenesis.

These embryonic shells also provide information about the microstructure of the shell wall, septa, and siphuncle. For example, the microstructure of the septa is similar to that of septa in juveniles and adults. Cements composed of prismatic crystals occur adapical of the junction of a septum and the outer shell wall. Such structural similarities may suggest similarities in secretory processes in embryogenesis and later ontogeny.

Finally, study of these embryonic shells disproves the existence of an organic protoconch attached to the cicatrix as postulated by Hyatt (1894). Instead, the cicatrix represents the site of initial shell formation. This feature occurs on the embryonic shells of all *Nautilus* species (Arnold et al., 1987). It has also been observed on the embryonic shells of Paleozoic nautiloids, suggesting its widespread occurrence in this group.

REFERENCES

Arnold, J. M.
1987. Reproduction and embryology of *Nautilus*. *In* W. B. Saunders and N. H. Landman (eds.), *Nautilus*: the biology and paleobiology of a living fossil, pp. 353–372. New York: Plenum Press.
1988. Some observations on the cicatrix of *Nautilus* embryos. *In* J. Wiedmann and J. Kullmann (eds.), Cephalopods—present and past, pp. 181–190. Stuttgart: Schweizerbart'sche Verlagsbuchhandlung.

Arnold, J. M., and B. A. Carlson
1986. Living *Nautilus* embryos: preliminary observations. Science 232: 73–76.

Arnold, J. M., N. H. Landman, and H. Mutvei
1987. Development of the embryonic shell of *Nautilus*. *In* W. B. Saunders and N. H. Landman (eds.), *Nautilus*: the biology and paleobiology of a living fossil, pp. 373–400. New York: Plenum Press.

Blind, W.
1976. Die ontogenetische Entwicklung von *Nautilus pompilius* (Linné). Palaeontographica 153: 117–160.

Grégoire, C.
1987. Ultrastructure of the *Nautilus* shell. *In* W. B. Saunders and N. H. Landman (eds.), *Nautilus*: the biology and paleobiology of a living fossil, pp. 463–486. New York: Plenum Press.

Hyatt, A.
1894. Phylogeny of an acquired characteristic. Proc. Am. Philos. Soc. 32: 349–747.

Mutvei, H.
1964. On the shells of *Nautilus* and *Spirula* with notes on the shell secretion in non-cephalopod molluscs. Ark. Zool. 16: 221–278.
1972. Ultrastructural studies on cephalopod shells. I. The septa and siphonal tube in *Nautilus*. Bull. Geol. Inst. Univ. Uppsala, n. ser., 3: 237–261.

Saunders, W. B., and N. H. Landman (eds.)
1987. *Nautilus*: the biology and paleobiology of a living fossil. New York: Plenum Press.

THIS PUBLICATION IS PRINTED ON ACID-FREE PAPER.